Petrology and Geochemistry of Scandium in Wailukum Ni Laterites, East Halmahera, Indonesia

Abdul Bari * , Mega Fatimah Rosana , Euis Tintin Yuningsih , Ade Kadarusman , Rubima Aisha Yulman , Muhammad Chandra RM , Thaha Rizal Ulhaque

Posted Date: 9 February 2026

doi: 10.20944/preprints202512.1452.v2

Keywords: East Halmahera; Wailukum; ultramafic; laterite; scandium

 doi:10.20944/preprints202512.1452.v2

Article

Petrology and Geochemistry of Scandium in Wailukum Ni Laterites, East Halmahera, Indonesia

Abdul Bari [1,2,*], Mega Fatimah Rosana [1], Euis Tintin Yuningsih [1], Ade Kadarusman [3], Rubima Aisha Yulman [2], Muhammad Chandra RM [2] and Thaha Riza Ulhaque [2]

[1] Faculty of Geological Engineering, Padjadjaran University, Bandung, Indonesia, 40132
[2] PT. Antam Tbk. Jakarta, Indonesia, 12530
[3] AKA Geosains Consulting, Tangerang, Indonesia, 15311
* Correspondence: abdulbariikawangi@gmail.com

Abstract

The Wailukum area in North Maluku Province, Indonesia, is an ultramafic rock complex with a high degree of serpentinization. The mineral composition of ultramafic and mafic rocks strongly influences scandium (Sc) distribution and enrichment during lateritization. This study aims to analyze the element distribution, mineral composition, and rock identification in three types of geological materials in a lateritic profile which contains Sc, specifically bedrock, saprolite, and limonite. The analytical methods used are petrography, X-ray Diffraction (XRD), X-ray Fluorescence (XRF), and Inductively Coupled Plasma-Optical Emission Spectroscopy (ICP-OES). Results show that in the bedrock, Sc is mainly associated with clinopyroxene minerals such as augite and diopside. In the saprolite, Sc content decreases due to higher mobility but remains partly associated with clinopyroxene. In the limonite zone, Sc reaches maximum enrichment. Among rock types, gabbro contains the highest absolute Sc concentration (23.25 ppm in bedrock and up to 58.5 ppm in limonite), while wehrlite records the greatest enrichment ratio, with a 9.18-fold increase from bedrock to limonite. In contrast, gabbro shows the lowest enrichment ratio (2.52-fold) despite its high initial Sc content. These patterns indicate that Sc enrichment is controlled by clinopyroxene as the primary host in bedrock, its relative stability during weathering.

Keywords: East Halmahera; Wailukum; ultramafic; laterite; scandium

1. Introduction

Scandium (Sc) is a transition metal and has atomic number 21 and usually occurs as Sc^{3+} in nature, this metal element was found by Lars Fredrik Nilson in 1879 [1]. The International Union of Pure and Applied Chemistry classified Sc as rare earth element (REE), although Sc has different compatibility with other REE due to its ionic radius [2]. Unlike other REEs, Sc is a compatible element because of its common size with Mg^{2+} and Fe^{2+}, which allows it to substitute easily into major rock-forming minerals such as pyroxene and amphibole [2]. As a result, Sc concentrations are generally higher in mafic and ultramafic rocks. Pyroxenites contain highest Sc concentration (up to 75 ppm) whereas the mafic rocks contain around 30-40 ppm [3]. Several studies [3–8] confirm the close association between scandium and ultramafic rocks, particularly pyroxene and amphibole minerals, through isomorphic substitution of Al or Mg in the crystal lattice.

Previous research by [4] emphasized that during weathering, scandium is mobilized and concentrated in lateritic limonite horizons through residual enrichment and an affinity for iron oxides, particularly goethite. Its concentration can increase significantly from approximately 15 ppm in basement rocks to approximately 81 ppm in limonite. The primary controlling factors for scandium accumulation are the type of basement rock and its host minerals. In fresh peridotite rocks, pyroxene

 doi:10.20944/preprints202512.1452.v2

is the dominant host, while in mafic-ultrabasic intrusions, hornblende plays the primary role. In laterite profiles, goethite plays a crucial role in the formation of scandium-rich zones.

Studies from [3,7] also show that the distribution of scandium in pyroxene is influenced by temperature, magma composition, and crystallization sequence. These studies further seek to identify which specific types of pyroxene host higher concentrations of scandium, with the results indicating that clinopyroxene is the primary host.

Present day Halmahera is interpreted as the result of double subduction system between Maluku Sea with Sangihe Arc in the west and Halmahera Arc in the east, this phenomenon subducted almost the entirety of the Maluku Sea and resulted in the emergence of the obducted ophiolite complex in the east of Halmahera Island [9] (Figure 1A). The Wailukum area is located in the East Halmahera geological province, which is characterized by an ophiolite complex and Mesozoic deep-sea sediments, imbricated with Paleogene sediments, and overlain by marine clastic sediments and Neogene carbonates (Figure 1B). The northeast arm of Halmahera Island where Wailukum area belongs, consists of dismembered ultramafic-mafic rocks complex with variable low-grade metamorphic overprint and intercalated with Mesozoic and Eocene sediments [10].

Based on local geological mapping by [11], the lithology types in the Wailukum area consists of mixed (melange) rocks, peridotite, partially serpentinized peridotite, and serpentinite lithological units (Figure 1C). The peridotite unit occupies >60% of the study area, stretching from the north to the south. Some of the peridotite has undergone quite strong serpentinization, and serpentinized peridotite extends to the southeastern part of the study area. In the northeastern part, a melange lithology extends northwest-southeast, directly adjacent to the peridotite. This unit is mixed within the shear zone and is exposed on the Wailukum ridge. Serpentinite is found in the central part of the study area and occupies approximately 10% of the study area. This unit is equated with the Cretaceous ultramafic rock unit [12]. From previous results by [11], the ultramafic complex in Wailukum, North Maluku, is estimated to contain significant amounts of scandium. This study aims to analyze the relationship between ultramafic rock type and scandium content through mineralogical studies of three geological horizons: bedrock, saprolite, and limonite.

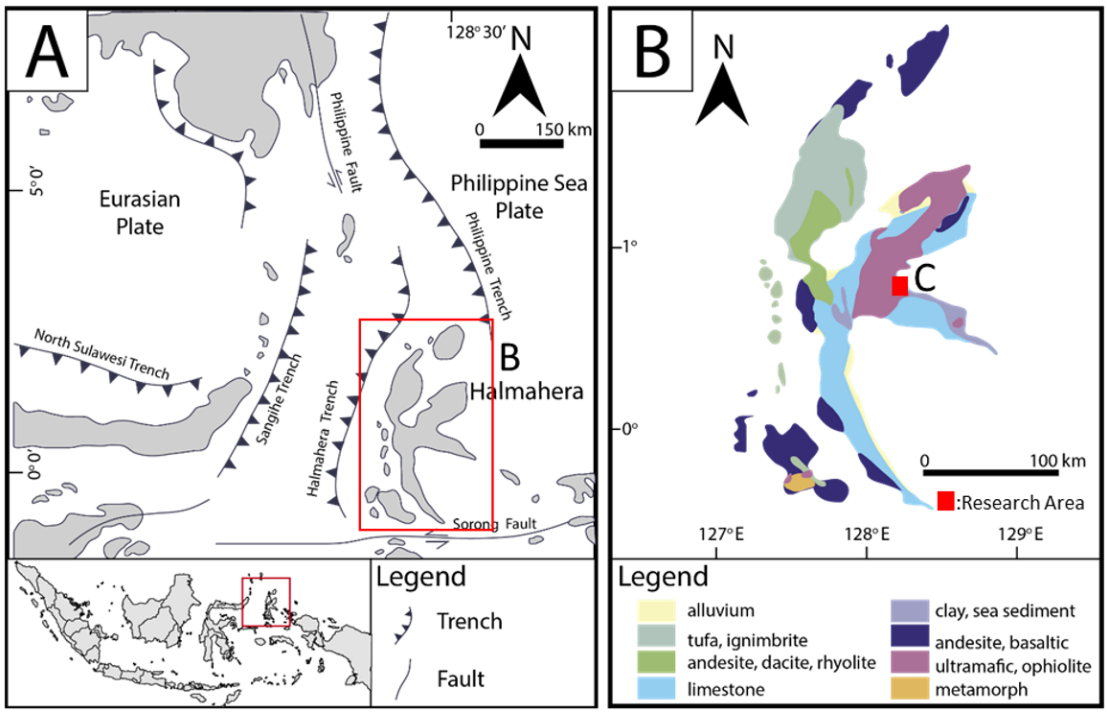

 doi:10.20944/preprints202512.1452.v2

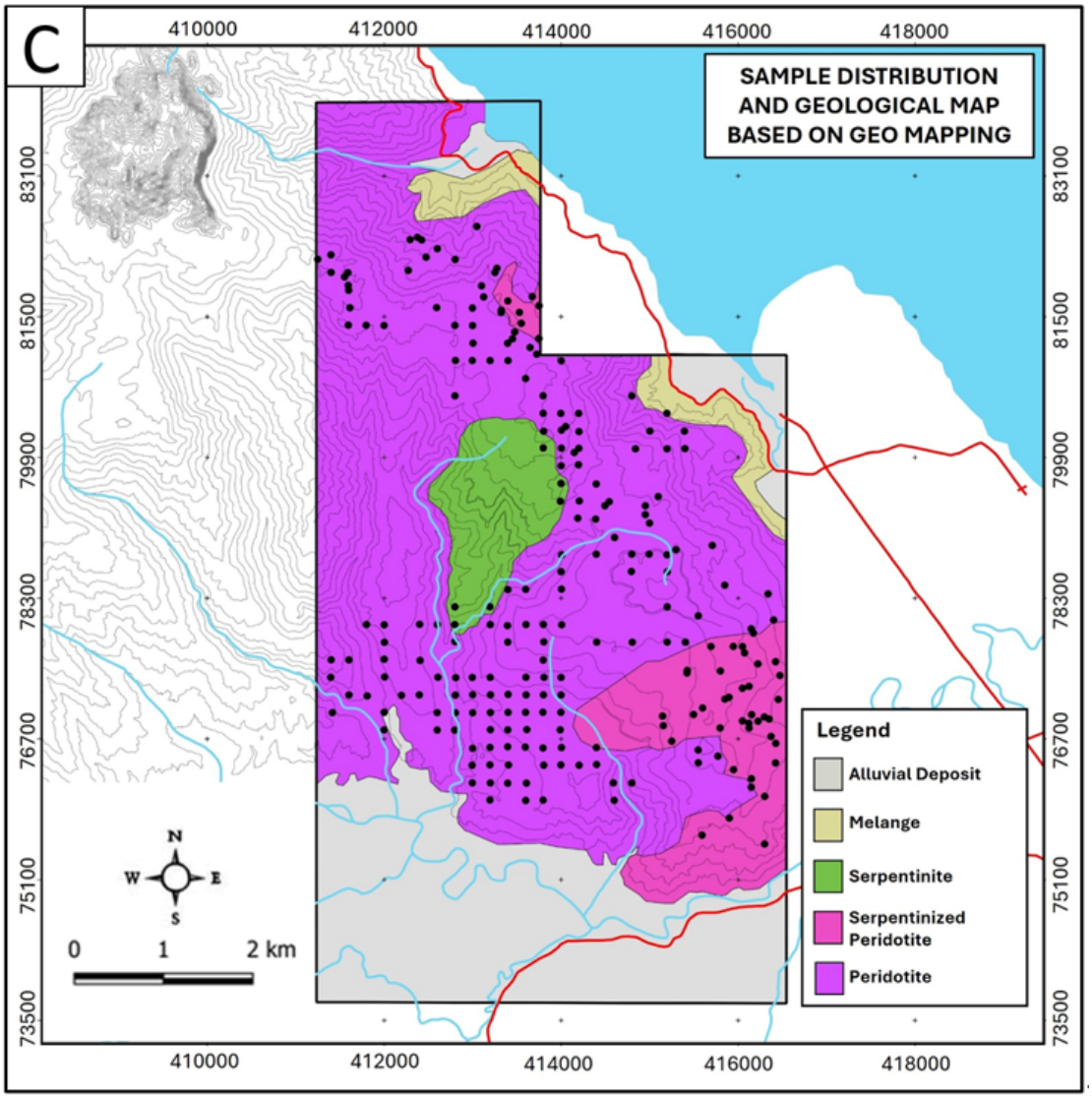

Figure 1. A. Regional tectonic setting of Halmahera and surrounding region [9]; B. Regional geology of Halmahera Island [10]; C. Local geological map of the Wailukum research area and location of sampling points from drill data [11].

2. Materials and Methods

This research was conducted through direct field data collection involving geological mapping and core drilling across the Wailukum area, North Maluku, Indonesia (Figure 1C). A total of 712 samples were collected from 270 drill holes, encompassing bedrock, saprolite, and limonite horizons. Among these, 231 bedrock samples from 270 drill points were selected for detailed petrographic and geochemical analyses to serve as the basis for lithological classification and rock distribution mapping within the study area.

Bedrock samples are characterized by fresh, hard, and unweathered lithologies that retain their primary mineral textures and structures. Saprolite samples represent the transitional weathering zone, where the original rock texture is partially preserved but the material is friable, with a light brown to yellowish coloration and reduced hardness (can be scratched by a knife; Mohs <3). Limonite samples correspond to the highly weathered upper zone, consisting of earthy to massive Fe-rich material with reddish-brown color, lacking recognizable primary texture, and containing abundant

 doi:10.20944/preprints202512.1452.v2

Fe-oxyhydroxides such as goethite and hematite. These field-based criteria ensure consistent identification and sampling of the three weathering zones across all drill samples.

Core sampling was conducted using the single-tube drilling method, with whole core sampling taken at 1-meter intervals. Core samples were NQ in size (~75.7 mm). Each drill data set was sampled at intervals representing each zone. These zones are distinguished by the degree of rock weathering, namely limonite, saprolite, and bedrock zones.

A total of 712 samples from 270 drill holes were prepared through preparation process using jaw crusher and pulverizer to obtain a representative #200 mesh pulp sample. Laboratory analysis was conducted at PT Aneka Tambang Tbk.'s internal laboratory and the Intertek Laboratory using X-Ray Fluorescence (XRF), Inductively Coupled Plasma – Optical Emission Spectroscopy (ICP-OES), and X-Ray Diffraction (XRD) methods, as well as at the Geoservices Laboratory using Scanning Electron Microscope – Energy Dispersive Spectroscopy (SEM-EDS).

The method used for petrographic analysis begins with preparing a thin section by cutting a rock slab (3 × 3 cm), grinding it to about 30 μm thickness so silicate minerals show their optical properties, and mounting it on a glass slide with adhesive and a coverslip. The thin section is then examined under a polarized light microscope Olympus BX51 and Nikon Eclipse LV100 Pol. This method allows identification of mineral types, estimation of their relative abundances, and observation of textural relationships such as grain size, shape, and arrangement.

XRD analysis using a Bruker D8 Advance instrument identified mineral composition based on X-ray diffraction patterns. The diffraction data were analyzed against the International Centre for Diffraction Data (ICDD) 2022 database using diffract. EVA v6.1 and Topaz v6.1 software. The results were calculated using the Rietveld refinement approach to quantify mineral phases, particularly in laterite samples that had undergone advanced weathering.

The XRF method using the Panalitycal Axios Fast Wavelength Dispersive X-Ray Fluorescence (WDXRF) instrument produced quantitative data on major elements in oxide form, such as Fe_2O_3, SiO_2, MgO, CaO, MnO, Cr_2O_3, Al_2O_3, P_2O_5, SO_3, also in base metal form, such as Ni and Co. The detection limit of each element is 0.15 wt%, 0.01wt%, 0.10 wt%, 0.007 wt%, 0.009 wt%, 0.04 wt%, 0.07 wt%, 0.01 wt%, and 0.02 wt%, respectively. The ICP-OES method, a plasma-based analytical technique for detecting metallic elements in ppm units, was used to analyze minor elements, including the presence of scandium.

We also conducted quality assurance and quality control (QAQC) using standard OREAS 193, OREAS 194 and blank samples using silica sand to ensure the accuracy and precision.

3. Results

3.1. Mineralogy Observations

3.1.1. Petrographic Analysis

Petrographic analysis on several samples shows at least three lithologies were identified on the research area namely dunite, serpentinite, and harzburgite.

Dunite is a type of ultramafic igneous rock consisting of olivine as the main mineral in rock formation, the presence of this mineral can reach 90% of the total minerals present in the rock. In the research area, the condition of this rock is generally dark gray-brownish (Figure 2A-B), there are many fractures or cracks, the dominant composition is olivine with medium to coarse mineral size, granular, has a low magnetic response, some of these fractures are filled by serpentine and form a mesh texture. The results of microscopic observation on this dunite rock show the presence of serpentinization from moderate to high, phaneric with medium to coarse mineral sizes (0.2 – 2 mm), holocrystalline, subhedral to euhedral, with the main mineral composition of olivine, with orthopyroxene mineral accessories, and a high degree of fracture, showing a mesh texture together with serpentine (Figure 2C-D).

 doi:10.20944/preprints202512.1452.v2

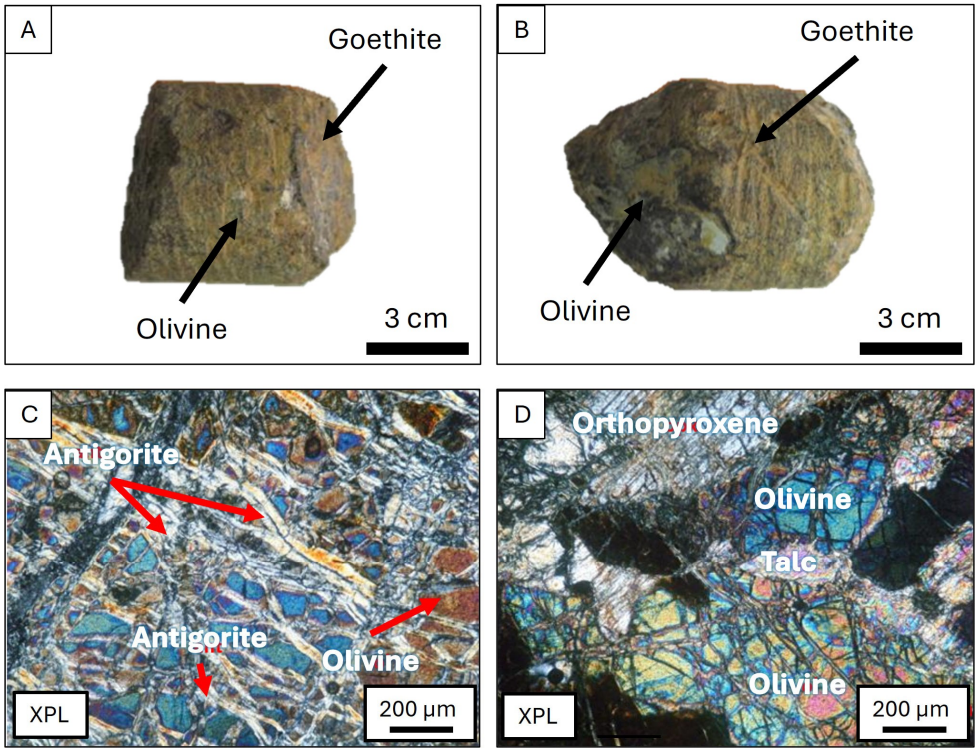

Figure 2. A-B. Handspecimen photo of dunite; C-D. photomicrocraph of coarse-grained olivine and accessory orthopiroxene. Olivine exhibits numerous fractures that have been transformed into antigorite (serpentine).

In the southeastern part of the observation area, a group of serpentinite rocks was observed. This rock is light green to dark green, which is characterized by whitish fractures fillings (Figure 3A). Serpentine, a holocrystalline, equigranular, fine-grained, fibrous mineral, consists of serpentine that alters the entire sample, and this mineral is also present as fracture fill materials that cut through this rock. Chlorite locally occurs as a selvage mineral along the serpentine veinlets (Figure 3B). The presence of serpentine minerals in each rock group is quite high, but in serpentinite-type rocks, they are grouped based on the occurrence of altered mineral more than 90% of total minerals.

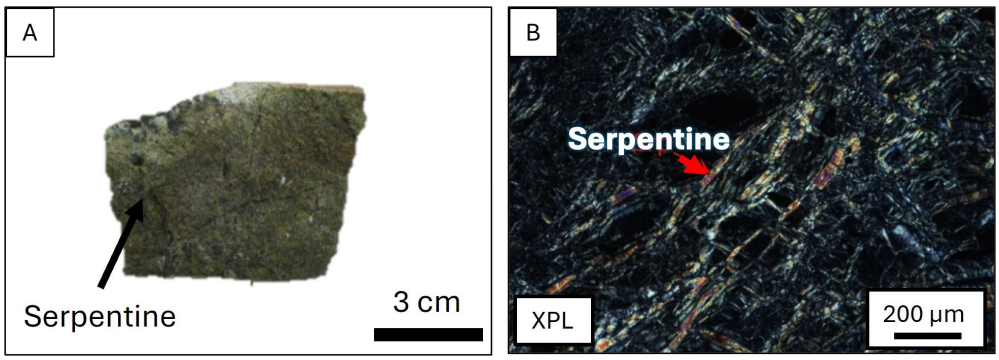

Figure 3. A. Handspecimen photo of serpertinite; B. Photomicrograph of fibrous serpentine.

Harzburgite found in the research area has dark green to brownish gray, composed predominantly of olivine, pyroxene, and in many cases, partially altered to serpentine. It has a medium to coarse granular texture with abundant fractures, phaneritic texture, and relatively low magnetic response. The serpentine mineral filled the fractures, producing a mesh texture typical of altered peridotites (Figure 4A-B).

 doi:10.20944/preprints202512.1452.v2

Under the microscope, the primary minerals observed in the serpentinite rock are olivine and orthopyroxene. These primary minerals are highly fractured and are partially filled by serpentine, which formed as an alteration product of both olivine and orthopyroxene. Serpentine is abundant in this rock, constituting more than 70% of the total mineral content. Microscopic observations (Figure 4C–F) reveal intensely fractured olivine and orthopyroxene with serpentine developed along fractures and weak planes within these primary minerals. Under reflected light, the occurrences of iddingsite are present locally, indicating partial alteration of olivine. In addition, chromite minerals are also observed with low abundance.

Olivine characterized by its colorless appearance, high relief, 2nd to 3rd order of birefringence, and a high density of fracture, that slightly replaced by serpentine. Orthopyroxene appears colorless to greenish with weak reddish pleochroism, high relief, 2nd to 3rd order of birefringence, and single direction cleavage. Fibrous serpentine occurs as a secondary mineral and filling fractures. Relict textures of the primary minerals are locally preserved, while serpentinization commonly occurs with a characteristic of mesh texture. Another alteration mineral observed is talc, which is colorless, has high-order birefringence, and low relief. Talc occurs in minor amounts, replacing primary minerals. Iddingsite is also present in minor quantities as iron oxide alteration products, appearing as reddish-brown patches replacing olivine. Chromite occurs as small, disseminated grains between olivine and orthopyroxene; in reflected light, it displays a skeletal form with a brownish tint in minor abundance. (Figure 4C-F).

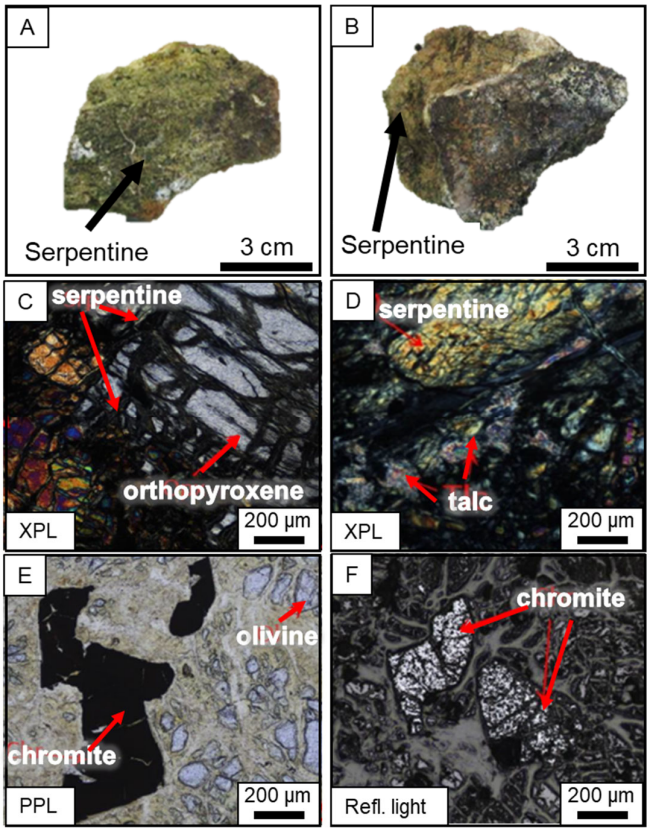

Figure 4. A-B. Hand specimen photo of harzburgite; C-F. Photomicrograph of harzburgite rocks in the basement zone.

3.1.2. XRD Analysis

On the basis of XRD analysis, there are at least 6 identified patterns based on the consistent variations of mineral spectrum (Figure 5). Type 1 spectrum is characterized by the occurrence of talc,

 doi:10.20944/preprints202512.1452.v2

forsterite, fayalite, diopside, enstatite, kaolinite, lizardite, and chlorite (Figure 5A). The X-ray diffraction pattern for sample BL31701 (Type 1) displays a complex assemblage of crystalline phases, as indicated by a series of well-defined peaks distributed between 5° and 60° 2θ. The diffraction profile is characterized by several high-intensity reflections, most notably the dominant peak near 11–12° 2θ and additional strong spectrum at approximately 25°, 36°, and 38° 2θ. These primary peaks suggest the presence of a mixed silicate mineralogy typical of serpentinized ultramafic lithologies. Overlaying the measured pattern are reference peak positions for eight candidate minerals: forsterite, fayalite, diopside, enstatite, kaolinite, lizardite, talc, and chlorite. Peak correspondence indicates that multiple phases contribute to the overall diffraction signal. The forsterite–fayalite series is represented by peaks in the 10–12° and 35–37° regions, consistent with Mg-Fe olivine components. Pyroxenes (diopside and enstatite) exhibit diagnostic reflections clustered between 28–32° and 36–40° 2θ, aligning closely with several medium-intensity peaks in the measured spectrum. Low-temperature alteration minerals—including lizardite, talc, and chlorite—are identified by characteristic peaks between ~7–10°, 18–20°, and 24–26° 2θ, corresponding with observed broad and moderate-intensity features. The presence of kaolinite is suggested by minor reflections near 12° and 24°. The combined pattern reflects partial serpentinization and hydrothermal alteration of a primary ultramafic protolith, producing an assemblage of olivine-pyroxene relicts overprinted by sheet silicates and hydrous Mg-phases.

Type 2 spectrum is characterized by the occurrence of talc, forsterite, fayalite, augite, diopside, enstatite, kaolinite, lizardite, talc, and tremolite (Figure 5B). The X-ray diffraction (XRD) pattern of sample BL85447-O (Type 2) illustrates the strongest reflections occur between ~28° and 38° 2θ, where overlapping peaks from orthopyroxene- and clinopyroxene-group minerals (augite, diopside, enstatite) coincide with olivine-group phases (forsterite, fayalite). Additional peaks at lower angles (~8°–15° 2θ) correspond to phyllosilicate minerals (kaolinite, lizardite, talc), indicating the presence of alteration products.

Type 3 spectrum is characterized by the occurrence of forsterite, fayalite, diopside, enstatite, kaolinite, lizardite, talc, and chlorite (Figure 5C). the X-ray diffraction (XRD) pattern of sample BL86369-Q (Type 3) shows the distribution of diffraction peaks associated with major silicate and phyllosilicate mineral phases. Prominent peaks occur at approximately 10°–12° 2θ and 25°–35° 2θ, where phyllosilicate minerals such as chlorite and serpentine-group phases produce their characteristic and high-angle reflections. Additional sharp peaks between ~30° and 40° 2θ are consistent with pyroxene minerals (augite, diopside, enstatite), suggesting the presence of relatively unaltered mafic silicate components.

Type 4 spectrum is characterized by the occurrence of forsterite, fayalite, kaolinite, lizardite, talc, and chlorite (Figure 5D). the X-ray diffraction (XRD) pattern of sample BL86466-O (Type 4) reveals strong reflections occur in the 28°–36° 2θ range, where the overlap of pyroxene-group minerals (augite, diopside, enstatite) contributes to multiple coincident peaks. Additional peaks at ~10°–12° 2θ correspond to basal spacings of chlorite and serpentine minerals, indicating the presence of alteration phases. Higher-angle reflections extending beyond 40° 2θ further support a heterogeneous composition containing both Mg-Fe silicates and phyllosilicates.

Type 5 spectrum is represented for samples that exhibit a high abundance of plagioclase. XRD analysis indicates the presence of feldspar (anorthite), pyroxenes (diopside and augite), serpentine (lizardite), and clay minerals, including kaolinite and chlorite (Figure 5E). Based on this mineral assemblage, these samples are classified as gabbro.

The final XRD pattern shows dominant lizardite with minor talc and chlorite (Figure 5F). This mineral assemblage indicates serpentinite, reflecting the high abundance of serpentine and associated alteration minerals commonly found in serpentinite rocks.

From these patterns, we also used the Rietveld refinement (Figure A1) approach to quantify mineral phases which then we plot the data to Streickesen diagram (1976) (Figure 6) [13]. Based on this analysis, Type 1 samples are classified as dunite, Type 2 as harzburgite, Type 3 as lherzolite, and Type 4 as wehrlite.

 doi:10.20944/preprints202512.1452.v2

3.1.3. XRD Data Application in the Mapping of the Ultramafic Complex

The initial geological maps, which were constructed through macroscopic observations and field surveys (Figure 1C) were substantially refined by integrating data from XRD and petrography analyses. As demonstrated in Figure 7, the updated maps delineate more detail lithological. The combined XRD and petrographic results reveal the presence of specific mineral subgroups, such as clinopyroxene and orthopyroxene minerals within the pyroxene group, that are not easily identified during the field or macroscopic observations [14,15].

It should be noted that most of the analyzed samples have undergone serpentinization and weathering, which may lead to uncertainty in mineralogical identification and quantitative phase estimation. Nevertheless, the XRD results obtained in this study remain valuable, as they preserve diagnostic mineralogical signatures that allow reasonable reconstruction of the protolith and identification of the original bedrock type, particularly when interpreted in conjunction with petrographic observations.

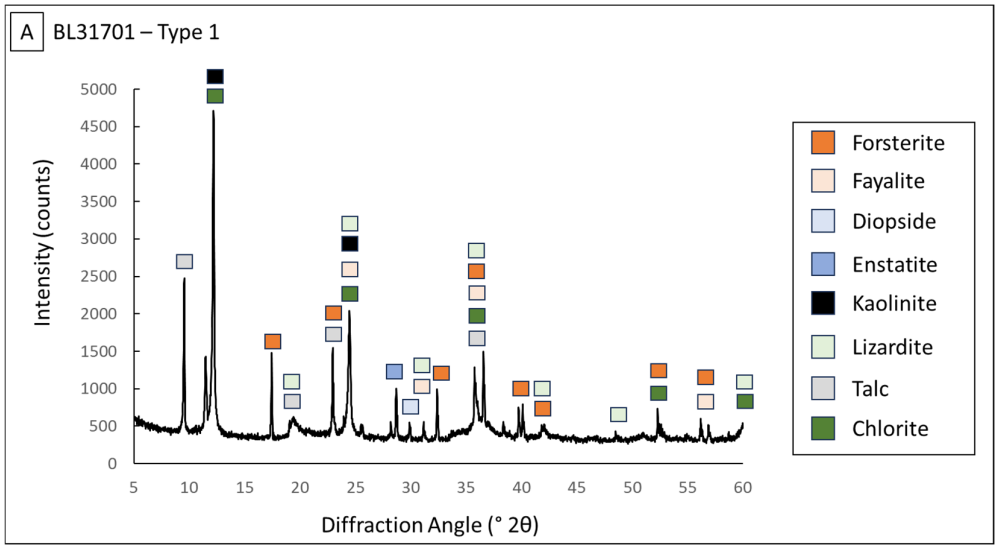

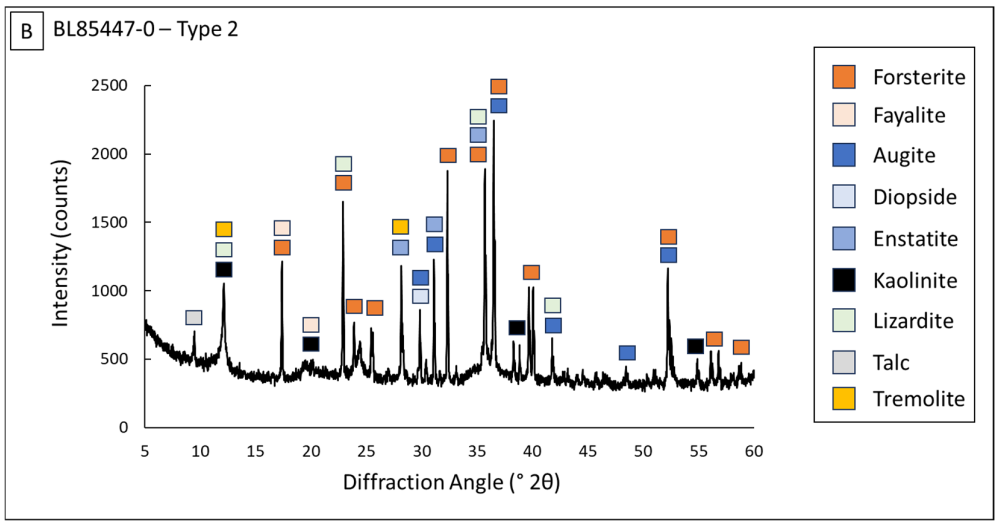

 doi:10.20944/preprints202512.1452.v2

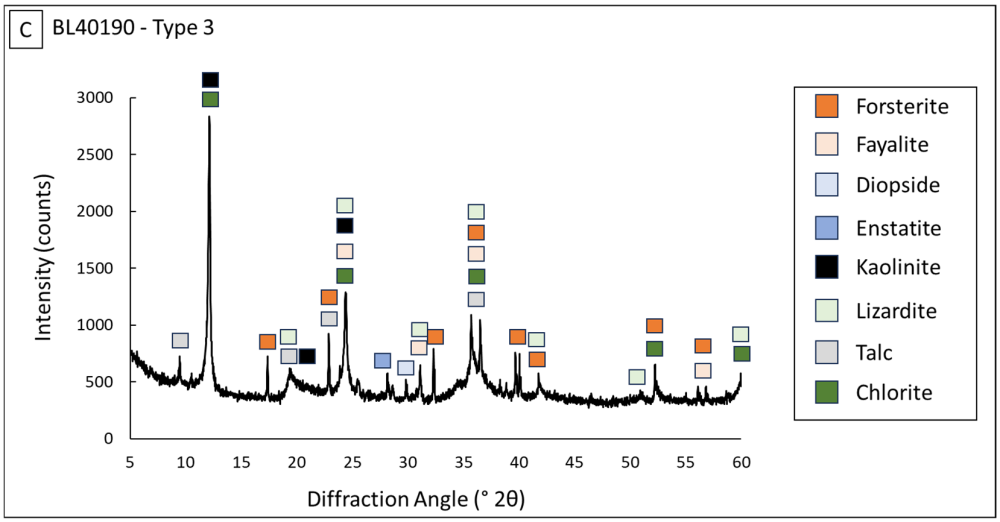

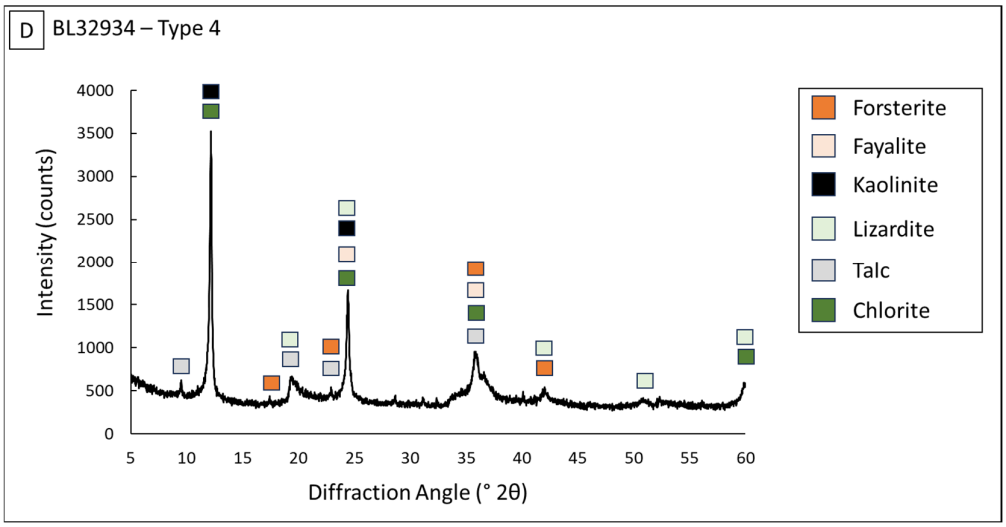

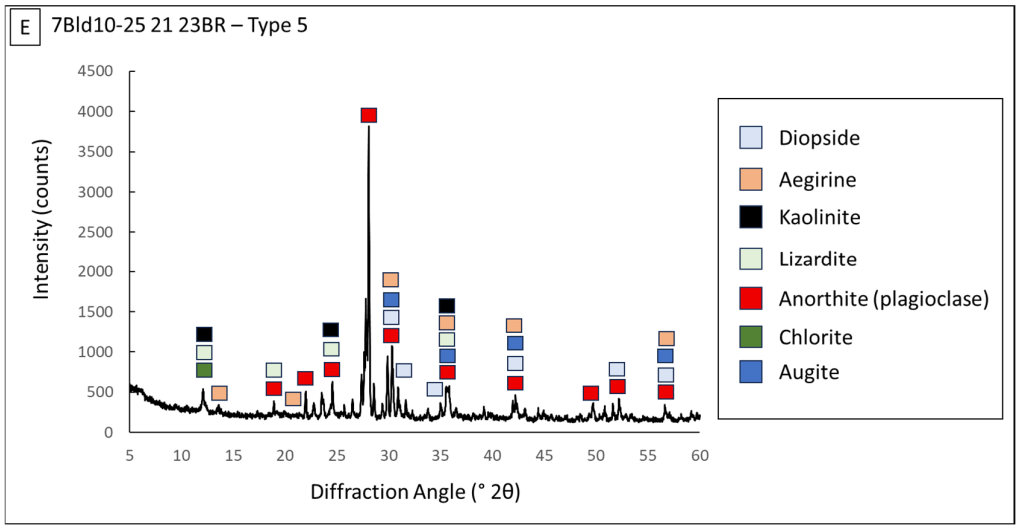

 doi:10.20944/preprints202512.1452.v2

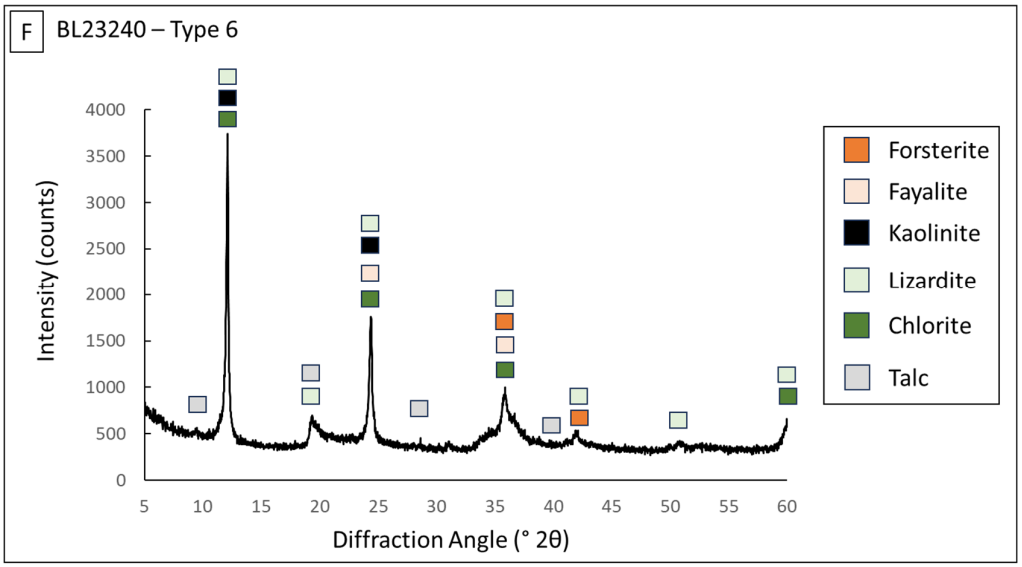

Figure 5. Representative of different types of XRD pattern in Wailukum research area: (A) dunite; (B) harzburgite; (C) lhezorlite; (D) wehrlite; (E) gabbro; (F) serpentinite**.** D-F Representative of different types of XRD pattern in Wailukum research area.

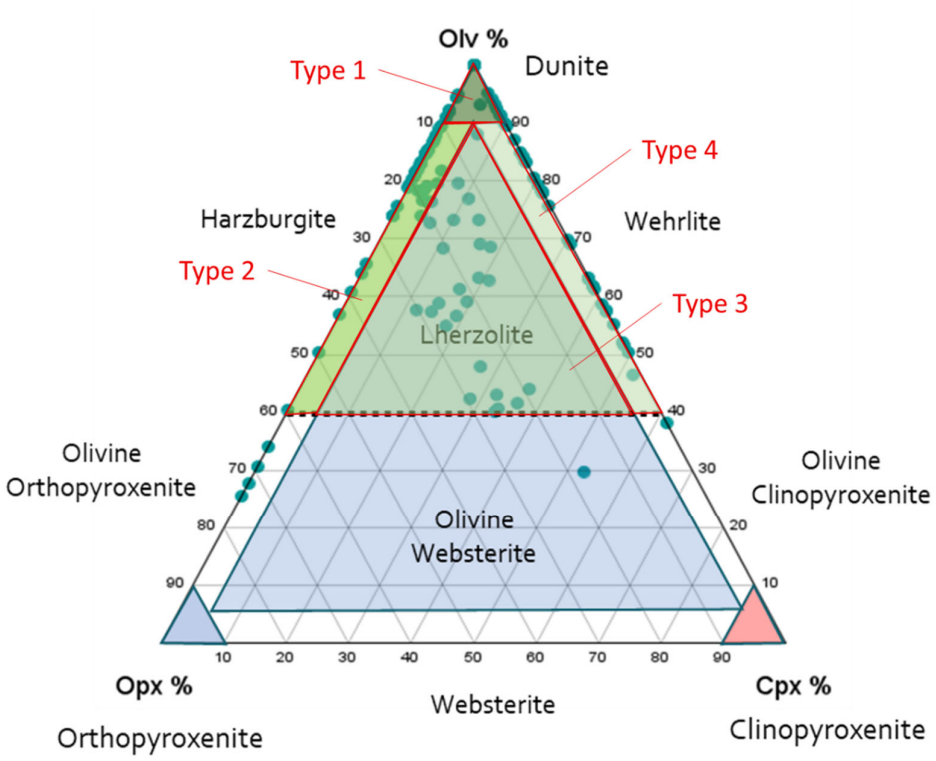

Figure 6. Distribution of bedrock types in the Wailukum area based on XRD analysis of bedrock, using Rietveld refinement method. Modified from [13].

 doi:10.20944/preprints202512.1452.v2

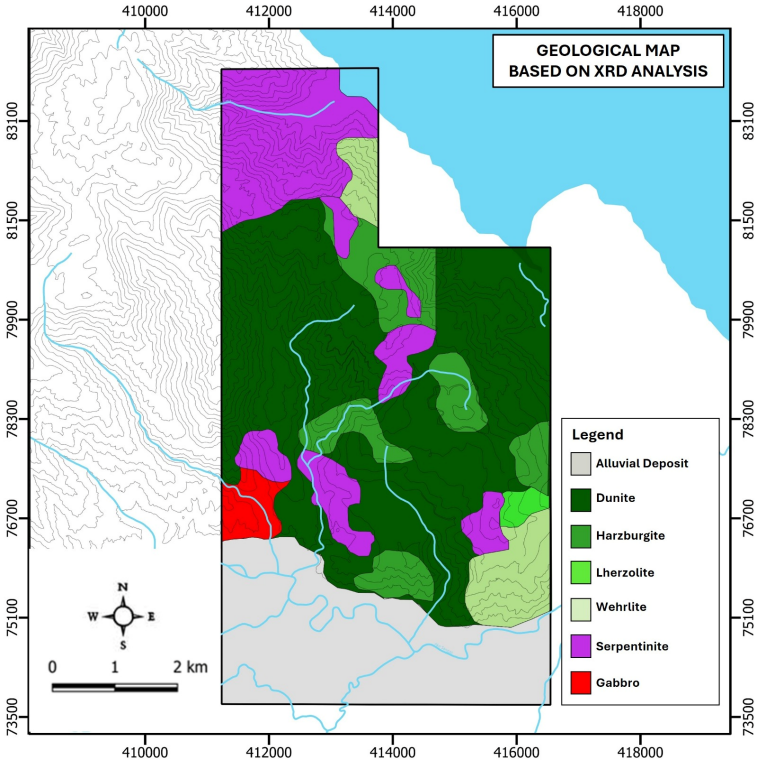

Figure 7. Geological map of the research area based on the results of XRD analysis.

3.2. Bulk Geochemistry

The results for bulk geochemical analysis using X-ray Fluorescence (XRF) and ICP-OES, which measures the overall concentration of major and trace elements in the rock, are summarized in Figure 8 and Table 1. The results indicate that scandium occurs with the highest intensity in gabbro, whereas the lowest degree of enrichment is observed in wehrlite, with an enrichment factor of 9.18 times in the limonite zone compared to the bedrock. Similarly, lherzolite shows an enrichment factor of 8.07 times in the limonite zone relative to the bedrock.

The geochemical composition of the ultramafic rock groups (dunite, harzburgite, lherzolite, serpentinite, and wehrlite) shows consistently low scandium concentrations (5.26–7.03 ppm) with broadly similar levels of Fe_2O_3 (7.70–8.42 wt%), SiO_2 (38.66–43.50 wt%), and MgO (38.69–40.03 wt%). Among them, harzburgite contains the highest scandium content (7.03 ppm), whereas wehrlite has the lowest (5.26 ppm). dunite is distinguished by its high MgO (40.03 wt%), consistent with its olivine rich mineralogy, while lherzolite and wehrlite record slightly higher CaO values (0.22–0.24 wt%), reflecting greater pyroxene proportions.

In contrast, the gabbroic bedrock exhibits a markedly higher geochemical signature for scandium, with an average concentration of 23.25 ppm, which is substantially elevated compared to the ultramafic groups. This abundance correlates with a significant increase in CaO (11.16%) and a corresponding decrease in MgO (16.01%), reflecting a primary mineralogy dominated by clinopyroxene.

Table 1. The composition of major elements in the rock groups in the Wailukum area and their comparison with the scandium and nickel levels in the bedrock zone.

Rock Groups	Laterite Zone	Sampel Quantity	Average Composition					
			Scandium (ppm)	Ni (wt%)	Fe_2O_3 (wt%)	SiO_2 (wt%)	MgO (wt%)	CaO (wt%)
Dunite	Limonite	42	44.55	0.98	49.14	9.60	4.66	0.06

 doi:10.20944/preprints202512.1452.v2

	Saprolite	34	18.95	1.77	18.13	33.13	24.86	0.08
	Bedrock	68	5.83	0.30	6.55	43.25	40.08	0.12
Harzburgite	Limonite	38	47.86	1.11	36.75	9.25	4.00	0.04
	Saprolite	28	14.29	1.55	9.51	39.67	26.97	0.14
	Bedrock	45	7.03	0.34	4.96	43.45	39.18	0.24
Lherzolite	Limonite	25	48.28	1.31	63.98	7.75	2.53	0.03
	Saprolite	25	12.09	1.69	16.48	36.51	28.92	0.11
	Bedrock	25	5.26	0.28	7.89	38.72	38.69	0.23
Wehrlite	Limonite	29	46.89	1.51	63.48	8.97	3.21	0.04
	Saprolite	26	12.27	2.08	15.20	37.35	29.82	0.08
	Bedrock	26	5.81	0.30	7.74	38.64	38.97	0.25
Serpentinite	Limonite	40	48.05	0.99	41.41	9.33	5.76	0.06
	Saprolite	33	19.28	1.55	22.62	31.27	24.92	0.05
	Bedrock	61	6.33	0.32	5.56	42.12	38.96	0.17
Gabbro	Limonite	2	58.50	0.57	45.67	15.65	3.76	0.20
	Saprolite	4	32.50	1.04	20.32	33.02	11.53	2.86
	Bedrock	4	23.25	0.11	6.30	38.93	16.01	11.16

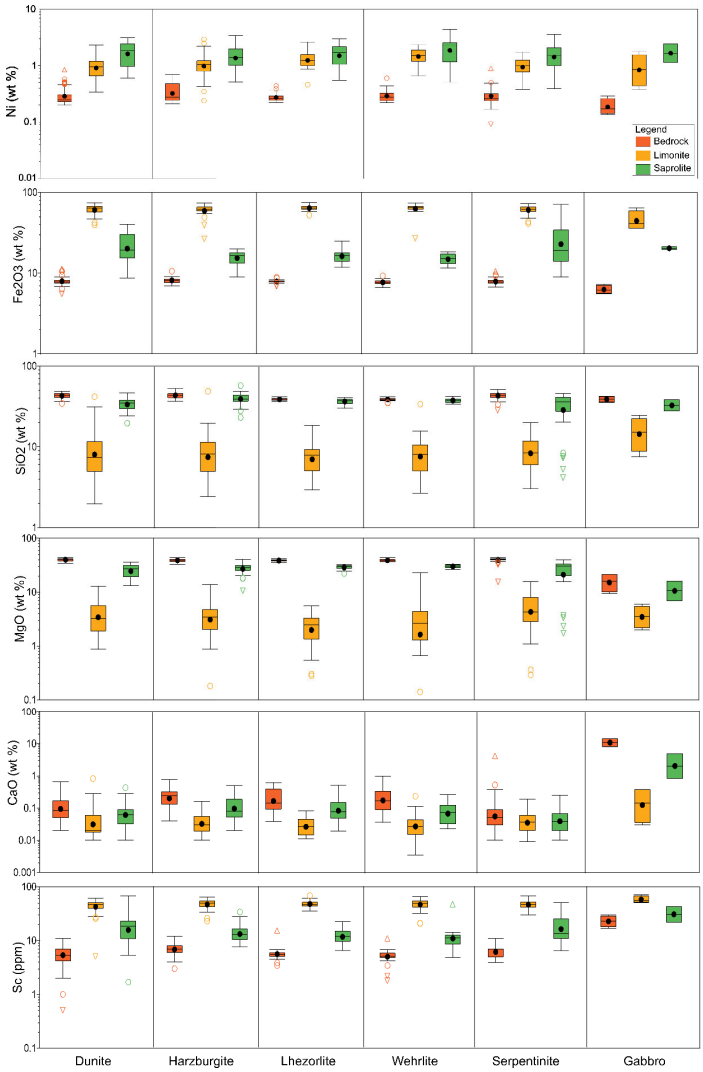

Figure 8. Representative XRF data of each horizon in Wailukum area.; the circle represents near outlier and the triangle represents far outlier.

 doi:10.20944/preprints202512.1452.v2

4. Discussion

4.1. The Importance of Protolith for Scandium Concentration

In the study area, an ultramafic igneous complex, scandium occurs in association with Fe-bearing minerals such as magnetite and clinopyroxene through the ionic substitution of Fe^{3+} by Sc^{3+}, facilitated by their comparable ionic radius (Sc^{3+} = 0.745 Å; Fe^{3+} = 0.645 Å) [16].

Mineralogical analyses indicate the presence of anorthite, and magnetite within ultramafic and gabbroic lithologies, where scandium incorporation is primarily controlled by magmatic crystallization processes, hydrothermal alteration, and the physicochemical conditions of the formation environment [17].

In primary ultramafic basement rocks such as dunite, harzburgite, wehrlite, lherzolite, which are characterized by low clinopyroxene abundance, the scandium content is typically 5–8 ppm, increasing to as much as 23 ppm in gabbroic rocks. This enrichment reflects the critical role of clinopyroxene in hosting scandium during magmatic solidification [17]. In Wailukum area, the order of Sc concentation in bedrock from the lowest to the highest are lhezorlite < wherlite < dunite < serpentinite < harzburgite < gabbro. The pattern shows different order with ultramafic complex in the eastern Australia where the order is dunite < peridotite < gabbro/basalt < amphibolite/pyroxenite [18].

In the Wailukum area, ultramafic lithologies such as lherzolite and wehrlite are characterized by relatively low proportions of clinopyroxene, largely because most samples have undergone extensive serpentinization and subsequent intense chemical weathering. The pronounced weathering of the bedrock is likely cause by the high abundance of serpentine minerals, which are prone to weathering. As a result, scandium originally hosted in primary clinopyroxene, one of the more weathering-resistant primary minerals, is only weakly retained in the bedrock. This process leads to comparatively low scandium concentrations in serpentinized lherzolite and wehrlite relative to dunite. (Figure 8).

In contrast, ultramafic complexes in eastern Australia display a different Sc trend due to variations in parent magma chemistry and metamorphic overprinting [18]. There, scandium enrichment is commonly associated with Fe–Ti oxide minerals in more evolved basaltic and amphibolitic lithologies rather than in peridotitic units. The divergence in the Wailukum sequence therefore underscores the importance of local magmatic evolution, and intensity of lateritic weathering in governing Sc distribution.

As for the serpentinite bedrocks in the Wailukum area, it is suspected that the higher Sc concentration in serpentinite compared to dunite and lherzolite in Wailukum area suggests that these serpentinite rocks are most likely derived from scandium rich protolith, such as harzburgite, which leads to there is no influence of serpentinization degree to the Sc enrichment in the rocks as Sc is considered as inert during the serpentinization process [19]. Although further analysis is necessary to confirm whether the serpentinization process in the Wailukum area affect the Sc enrichment or not.

Overall, the observed pattern indicates that scandium distribution in the Wailukum complex is not solely controlled by primary mineralogy but also by the alteration activities, and secondary mineral formation during tropical laterization. This multi-stage control contrasts with the Australian systems, where igneous fractionation and metamorphic re-equilibration dominate scandium partitioning in the bedrock sequence.

4.2. Scandium Enrichment in Laterization Process

In the study area, scandium enrichment is strongly influenced by mineral stability during tropical weathering. Clinopyroxene and chromite within ultramafic bedrock exhibit greater resistance to lateritization compared to olivine, allowing scandium to remain bound to these more stable minerals within the saprolite zone. In lithologies such as dunite, harzburgite, and serpentinite, where olivine is abundant but highly unstable under tropical conditions, intense alteration releases

 doi:10.20944/preprints202512.1452.v2

Fe, Mg, and other mobile elements, while scandium remains structurally incorporated within residual clinopyroxene and chromite phases [18,20–22].

As weathering advances upward, Sc^{3+} is released from silicate lattices and remobilized through meteoric fluids percolating along fractures and pore spaces. The saprolite zone thus represents a transitional geochemical environment, where both residual and secondary processes govern scandium distribution. In this zone, Sc persists in association with clinopyroxene, chromite–spinel, magnetite, and asbolane [20]. In contrast, the limonite zone marks the dominance of secondary Fe–oxyhydroxide formation, where scandium is immobilized through adsorption or structural incorporation into goethite and hematite.

Quantitative assessment of scandium enrichment across the weathering profile reveals significant vertical and lithological variability (Figure 8). As summarized in Table 2, the average scandium concentration in the saprolite zone is 2.36 times higher than in bedrock, while the limonite zone shows an enrichment of 2.97 times relative to the saprolite. The cumulative enrichment from bedrock to limonite averages approximately 6.97 times.

Across lithologies, the enrichment factors are relatively consistent among ultramafic rocks but notably lower in gabbro. Although gabbro contains the highest primary scandium concentrations due to its clinopyroxene-rich composition, it displays limited secondary enrichment, suggesting that the resistance of gabbroic textures to intense weathering inhibits scandium remobilization and adsorption onto secondary phases. Conversely, ultramafic rocks such as serpentinite and harzburgite, which undergo extensive alteration and Fe-oxide formation, exhibit more pronounced scandium enrichment.

Elemental correlation analysis (Figure 9) shows that scandium enrichment in the lateritic profile closely parallels the distribution of Fe and Ni, confirming that Fe–oxide formation is the primary control on scandium mobility and fixation. Additionally, chromium (Cr) and manganese (Mn) display anomalous patterns that vary across lithologies.

In the saprolite zone, Cr and Mn contents are relatively low in gabbro, wehrlite, and lherzolite, but markedly higher in dunite and serpentinite, suggesting that Cr- and Mn-bearing secondary oxides may contribute locally to scandium retention. In the limonite zone, enrichment anomalies in Cr and Mn become more pronounced within gabbro, wehrlite, and lherzolite-derived profiles, indicating differential elemental migration and redox-controlled precipitation.

Overall, these elemental correlations confirm that scandium enrichment during lateritization is driven primarily by Fe–oxide accumulation, but modulated by rock composition, mineral stability, and redox dynamics during tropical weathering.

Table 2. The level of scandium enrichment in each laterite zone and rock group.

Dunite			**Harzburgite**		
Bedrock	Saprolite	Limonite	Bedrock	Saprolite	Limonite
5.83 ppm	18.95 ppm	44.55 ppm	7.03 ppm	14.29 ppm	47.86 ppm
S/B	L/S	L/B	S/B	L/S	L/B
3.25	**2.35**	**7.64**	**2.03**	**3.35**	**6.81**
Wehrlite			**Lherzolite**		
Bedrock	Saprolite	Limonite	Bedrock	Saprolite	Limonite
5.26 ppm	12.09 ppm	48.28 ppm	5.81ppm	12.27 ppm	46.89 ppm
S/B	L/S	L/B	S/B	L/S	L/B
2.30	**3.99**	**9.18**	**2.11**	**3.82**	**8.07**
Serpentinite			**Gabbro**		
Bedrock	Saprolite	Limonite	Bedrock	Saprolite	Limonite
6.33 ppm	19.28 ppm	48.05 ppm	23.25 ppm	32.5 ppm	58.5 ppm
S/B	L/S	L/B	S/B	L/S	L/B
3.05	**2.49**	**7.59**	**1.40**	**1.80**	**2.52**

(Note: S/B is the ratio between saprolite to bedrock; L/S is the ratio between limonite to saprolite; L/B is the ratio between limonite to bedrock).

 doi:10.20944/preprints202512.1452.v2

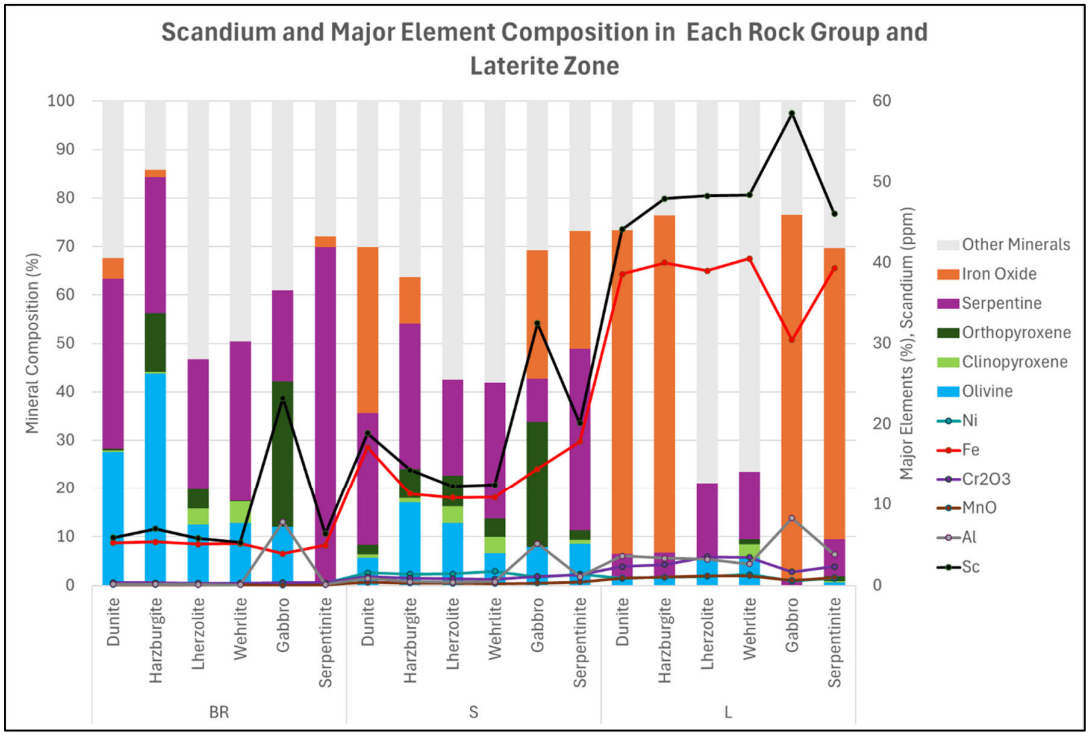

Figure 9. Scandium and major element composition in each rock group and laterite zone.

4.3. Implication for the Exploration in Wailukum Area

[17] reported that clinopyroxene-rich lithologies exhibit a high potential for scandium (Sc) mineralization, as intense chemical weathering can effectively liberate Sc from the protolith and promote its accumulation in the regolith. In the Wailukum area, such clinopyroxene-rich lithologies are primarily represented by lhezorlite, wehrlite, and gabbro units (Figure 7). Considering that scandium grades in known laterite deposits range from approximately 33 ppm in the Shazi deposit, China, to nearly 300 ppm in the Lucknow deposit, Australia [17] and [23,24], the scandium concentrations identified in Wailukum are ranging from 44.55 to 58.50 ppm, these results suggest that this area may hold significant potential for scandium deposit.

However, further detailed geochemical characterization and systematic exploration are required to delineate the most prospective zones and assess the resource potential accurately. In addition, bulk geochemical data (Figure 8) show a positive correlation between Sc, Ni, and Fe_2O_3, indicating that bulk Ni and Fe_2O_3 contents may serve as useful geochemical proxies for Sc enrichment. Nevertheless, additional investigations are needed to validate these relationships and establish a more robust geochemical indicator framework for scandium mineralization in the region.

5. Conclusions

Scandium distribution and enrichment within the Wailukum ultramafic complex are governed by a two-stage control system involving both primary magmatic processes and secondary supergene alteration. The protolith composition exerts a first-order influence on initial scandium abundance, with Sc hosted primarily in Fe-bearing minerals such as magnetite and clinopyroxene through Fe^{3+}–Sc^{3+} ionic substitution during late-stage magmatic differentiation. Among the ultramafic lithologies, Sc concentrations range from 5–8 ppm in dunite and lherzolite to up to 23 ppm in gabbro, reflecting the critical role of clinopyroxene in controlling primary Sc partitioning. However, the observed lithological sequence of Sc content in Wailukum (lherzolite < wehrlite < dunite < serpentinite < harzburgite < gabbro) diverges from that in eastern Australia, emphasizing the influence of local magmatic evolution and weathering intensity on Sc distribution.

 doi:10.20944/preprints202512.1452.v2

Overall, Sc enrichment in the Wailukum complex reflects an integrated magmatic–supergene system, where both primary mineralogical characteristics and secondary weathering processes govern scandium behavior. These findings not only elucidate the mechanisms of Sc mobility and fixation but also provide a predictive framework for exploration, emphasizing the importance of identifying serpentinite-rich and highly lateritized zones as the most prospective targets for Sc resource development in tropical ultramafic terrains.

Author Contributions: Conceptualization, A.B., M.F.R., E.T.Y., and A.K.; methodology, A.B.; software, M.C.R.M.; validation, A.B., M.F.R., E.T.Y., and A.K.; formal analysis, A.B, R.A.Y.; investigation, A.B., T.R.U.; writing—original draft preparation, A.B.; writing—review and editing, A.B, M.F.R., E.T.Y., and A.K.; visualization, A.B., R.A.Y., M.C.R.M., and T.R.U.; supervision, M.F.R., E.T.Y., and A.K; project administration, A.B.; funding acquisition, A.B. All authors have read and agreed to the published version of the manuscript.

Funding: This research was funded by PT Antam Tbk.

Data Availability Statement: All relevant data are in this paper.

Acknowledgments: We sincerely acknowledge **PT Antam Tbk** for granting permission and providing support for this research at the Wailukum area. We are grateful to the editor, **Astrid Yang**, for her constructive comments and guidance, and to the four anonymous reviewers for their insightful suggestions, which significantly improved the quality of the manuscript. Special thanks are extended to **Andi Kurniawan, Syaiful Hilal, Duduk Sumargono, Reza Rizqie Ramadhan, and Naafiakra Nouval** for their invaluable assistance during fieldwork and data analysis. This study was also generously supported by funding from **PT Antam Tbk**, which is gratefully acknowledged.

Conflicts of Interest: The research was conducted on the Wailukum area, owned by PT Aneka Tambang Tbk, with which Abdul Bari, Rubima Aisha Yulman, Muhammad Chandra RM, and Thaha Riza Ulhaq are affiliated. Although this affiliation may present a potential conflict of interest, the authors affirm that the research was conducted transparently, with adherence to ethical guidelines, and that every effort was made to maintain objectivity and minimize bias in the study design, data collection, analysis, and interpretation. The remaining authors declare no conflicts of interest.

 doi:10.20944/preprints202512.1452.v2

Appendix A

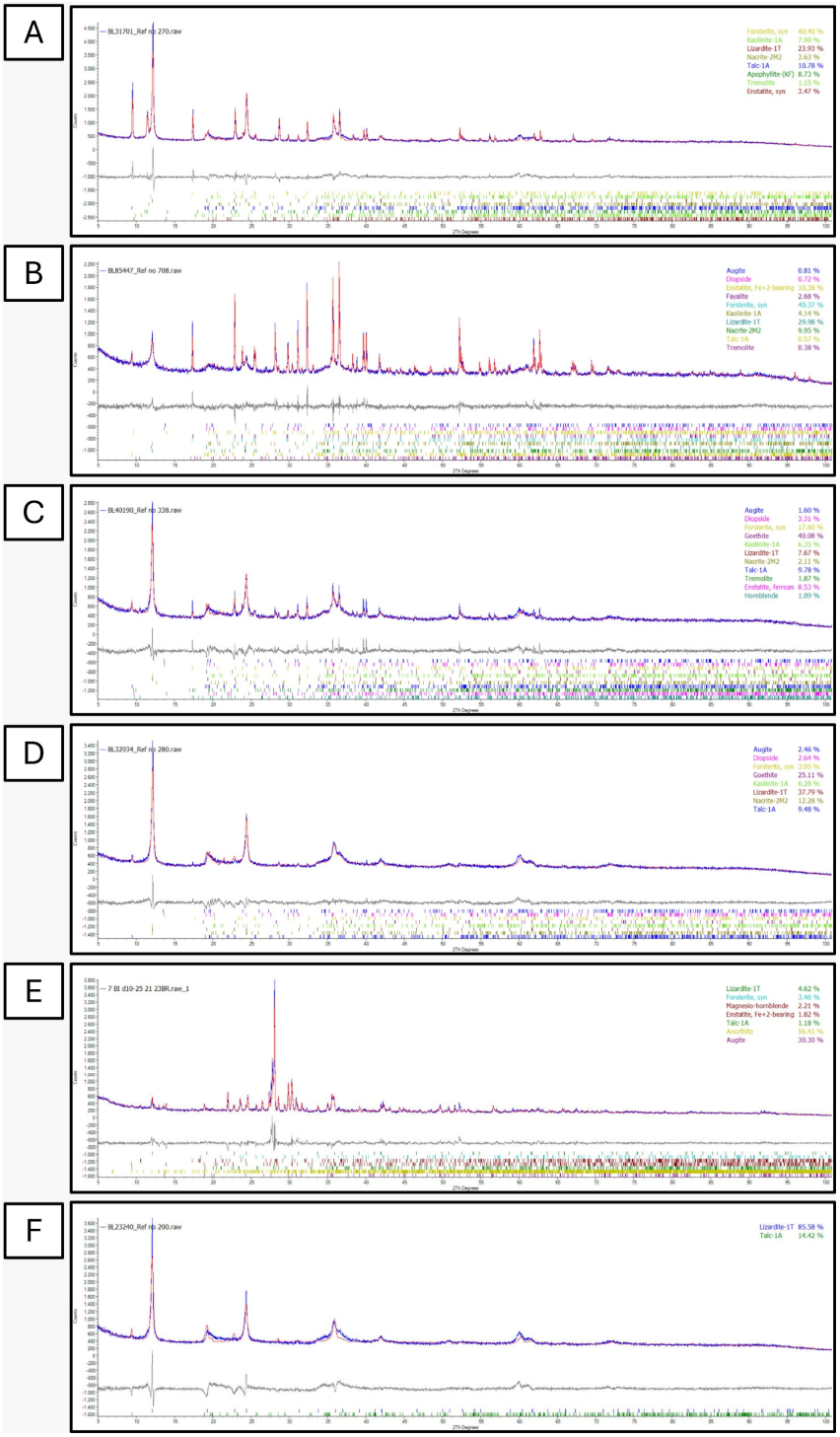

Figure 1. (A-F) Rietveld refinement for all type (type 1 – 6) XRD spectra in Wailukum, the blue line indicates raw sample line, red line indicates interpretation line, and black line indicates deviation line between raw sample with interpretation line.

 doi:10.20944/preprints202512.1452.v2

References

1. Iain, S. M., & Chassé, M. (2016). Scandium. *Encyclopedia of Geochemistry*, 1-4.
2. Williams-Jones, A. E., & Vasyukova, O. V. (2018). The economic geology of scandium, the runt of the rare earth element litter. *Economic Geology*, *113*(4), 973-988.
3. Kempe, U., & Wolf, D. (2006). Anomalously high Sc contents in ore minerals from Sn–W deposits: possible economic significance and genetic implications. *Ore Geology Reviews*, *28*(1), 103-122.
4. Onggang, S., Maulana, A., & Irfan, U. R. (2021). Preliminary Study of Scandium Enrichment in Lateritic Profile from Weathered Ultramafic Rock in Lapaopao Area Kolaka Regency of Southeast Sulawesi. IOP Conference Series: Earth and Environmental Science, 921(1), 012040.
5. Teitler, Y., Cathelineau, M., Ulrich, M., Ambrosi, J. P., Munoz, M., & Sevin, B. (2019). Petrology and geochemistry of scandium in New Caledonian Ni-Co laterites. Journal of Geochemical Exploration, 196, 131–155.
6. Chassé, M., Griffin, W. L., O'Reilly, S. Y., & Calas, G. (2016). Scandium speciation in a world-class lateritic deposit. Geochemical Perspectives Letters, 3(2), 105–114.
7. Maulana, A., Sanematsu, K., & Sakakibara, M. (2016). An overview on the possibility of scandium and REE occurrence in Sulawesi, Indonesia. Indonesian Journal on Geoscience, 3(2), 139–147.
8. Stueber, A. M., & Goles, G. G. (1967). Abundances of Na, Mn, Cr, Sc and Co in ultramafic rocks. Geochimica et Cosmochimica Acta, 31(1), 75–93.
9. Hall, R. (2000). Neogene History of Collision in The Halmahera Region, Indonesia. Proceedings of the Indonesian Petroleum Association 27th Annual Convention, 487-493.
10. Darman, H. (2000). An outline of the geology of Indonesia. Lereng Nusantara. https://books.google.com/books?hl=en&lr=&id=NyqDDwAAQBAJ&oi=fnd&pg=PP2&dq=Sukamto+et+al.,+1981+dalam+Darman+%26+Sidi,+2000&ots=UgvtDwCwqG&sig=M7u40Y5bu4x-wBCDlYz8jeBygww
11. Antam. (2023). Annual report – Nickel Laterite Exploration in East Halmahera, North Maluku, Indonesia. Internal report (unpublished manuscript).
12. Apandi, T. & Sudana, D. 1980. Geologic map of the Ternate quadrangle, North Maluku. Geological Research and Development Centre, Bandung, Indonesia.
13. Streckeisen, A. (1976). To each plutonic rock its proper name. *Earth-science reviews*, *12*(1), 1-33.
14. Sufriadin, Widodo, S., Jaya, A., & Azman. (2022, November). The effect of heating on mineral and chemical composition of saprolite ore from Latowu area, North Kolaka regency of Southeast Sulawesi, Indonesia. In *AIP Conference Proceedings* (Vol. 2543, No. 1, p. 050006). AIP Publishing LLC.
15. El Mendili, Y., Chateigner, D., Orberger, B., Gascoin, S., Bardeau, J. F., Petit, S., Duee, C., Le Guen, M. & Pilliere, H. (2019). Combined XRF, XRD, SEM-EDS, and Raman analyses on serpentinized harzburgite (nickel laterite mine, New Caledonia): Implications for exploration and geometallurgy. *ACS Earth and Space Chemistry*, *3*(10), 2237-2249.
16. Marsh, E. E., Anderson, E. D., & Gray, F. (2011). *Ni-Co Laterites: A Deposit Model*. Denver, CO: US Department of the Interior, US Geological Survey.
17. Wang, Z., Li, M. Y. H., Liu, Z. R. R., & Zhou, M. F. (2021). Scandium: Ore deposits, the pivotal role of magmatic enrichment and future exploration. *Ore Geology Reviews*, *128*, 103906.
18. Chassé, M., Griffin, W. L., O'Reilly, S. Y., & Calas, G. (2019). Australian laterites reveal mechanisms governing scandium dynamics in the critical zone. *Geochimica et Cosmochimica Acta*, *260*, 292-310
19. Teitler, Y., Cathelineau, M., Ulrich, M., Ambrosi, J. P., Munoz, M., & Sevin, B. (2019). Petrology and geochemistry of scandium in New Caledonian Ni-Co laterites. *Journal of Geochemical Exploration*, *196*, 131-155.
20. Qin, H. B., Yang, S., Tanaka, M., Sanematsu, K., Arcilla, C., & Takahashi, Y. (2021). Scandium immobilization by goethite: Surface adsorption versus structural incorporation. *Geochimica et Cosmochimica Acta*, *294*, 255-272.
21. Goldich, S. S. (1938). A study in rock-weathering. *The Journal of Geology*, *46*(1), 17-58.
22. Shepherd, K., Namur, O., Toplis, M. J., Devidal, J. L., & Charlier, B. (2022). Trace element partitioning between clinopyroxene, magnetite, ilmenite and ferrobasaltic to dacitic magmas: an experimental study on the role of oxygen fugacity and melt composition. *Contributions to Mineralogy and Petrology*, *177*(9), 90.

 doi:10.20944/preprints202512.1452.v2

23. Hoatson, D. M., Jaireth, S., & Miezitis, Y. (2011). The major rare-earth-element deposits of Australia: geological setting, exploration, and resources. Geoscience Australia.
24. Nie, A. G., Sun, J., & Zhang, M. (2018). Analysis of forming conditions and genesis of Sazi independent scandium deposit in Qinglong, Guizhou Province. *Journal of Guizhou University (Natural Sciences)*, *35*(5), 31-36.